RSC Advances

Theoretical Mechanistic Investigation of Zinc(II) Catalyzed Oxidation of Alcohols to Aldehydes and Esters

Journal:	*RSC Advances*
Manuscript ID	RA-ART-11-2015-023096.R2
Article Type:	Paper
Date Submitted by the Author:	28-Feb-2016
Complete List of Authors:	Nisa, Riffat; COMSATS, Chemistry Mahmood, Tariq; COMSATS, Institute of Information Technology, Ludwig, Ralf; Universitat Rostock, Institute fur Chemie Ayub, Khurshid; COMSATS Institute of Information Technology, Chemistry
Subject area & keyword:	Homogeneous < Catalysis

RSC Advcances

ARTICLE

Theoretical Mechanistic Investigation of Zinc(II) Catalyzed Oxidation of Alcohols to Aldehydes and Esters

Received 00th January 20xx,
Accepted 00th January 20xx

DOI: 10.1039/x0xx00000x

www.rsc.org/

Riffat Un Nisa[a], Tariq Mahmood[a], Ralf Ludwig[b,c], Khurshid Ayub*[a]

Mechanism of Zn(II) catalyzed oxidation of benzylic alcohol to benzaldehyde and ester by H_2O_2 oxidant is investigated through density functional theory methods, and compared with the similar oxidation mechanisms of other late transition metals. Both inner sphere and intermediate sphere mechanisms have been analyzed in the presence and absence of Pyridine-2- carboxylic acid (ligand). An intermediate sphere mechanism involving transfer of hydrogen from alcohol to H_2O_2 was found preferred over the competitive inner sphere mechanism involving β hdydride elimination. Kinetic barriers associated with the intermediate sphere mechanism are consistent with the experimental observations, suggesting that the intermediate sphere mechanism is a plausible mechanism under these reaction conditions. Oxidation of alcohols to aldehyde (first step) is kinetically more demanding than the oxidation of hemiacetals to esters (second step). Changing the oxidant to *tert*-butyl hydrogen peroxide (TBHP) increases the activation barrier for oxidation of alcohol to aldehyde by 0.4 kcal mol^{-1} but decreases the activation barrier by 3.24 kcal mol^{-1} for oxidation of hemiacetal to esters. Replacement of zinc bromide with zinc iodide causes the second step more demanding than the first step. Pyridine-2-carboxylic acid ligand remarkably decreases the activation barriers for the intermediate sphere pathway whereas a less pronounced inverse effect is estimated for the inner sphere mechanism.

Introduction:

Esters represent an important class of organic compounds, and find applications in in fine and bulk chemical industries, fragrances, essential oils, pheromones, pharmaceuticals, agrochemicals,[1] plastics and textile industries.[2] Conventional methods [3,4,5] to prepare esters generally involve tedious procedures, and produce toxic wastes[6]. Over the time, several sophisticated strategies have appeared in the literature to build the ester bond, mainly through transition metal catalysis[7–9].

More recently, palladium catalyzed direct oxidative cross esterification of benzylic and aliphatic alcohols to esters is reported independently by Beller[10] and Lei.[11] In the direct oxidative cross reaction, oxygen was used as an oxidant, and esters were prepared in good yields. The reaction involves oxidation of alcohol to aldehyde. The resulting aldehyde then reacts with anther molecule of alcohol to form hemiacetal which on further oxidation delivers the ester product. The reaction is environmentally benign with high atom economy without the need of any activating agent. The concept of oxidation (dehydrogenation) of alcohols is more than 100 years old (Guerbet Chemistry)[12] but its elegant use in ester [13] and amide[14] formation has not been realized until recently. Several other late transition metals have been used for similar oxidation reaction[10,11,13,15–24].

Since the catalysts used in the oxidative transformation (mostly Pd, Ir, Ru, Au) are expensive, therefore, the reactions are economically not viable, particularly on industrial scale. An important factor in the large scale utilization of these reactions is the cost of the catalyst therefore; research is more focused recently towards exploration of cheap, non-toxic and environmentally benign catalysts, particularly those based on bio-relevant metals, such as iron, zinc, and copper. In this regard, Yefeng Zhu et. al. have reported a copper metal based catalyst for selective oxidation of alcohols to ester. Selectivity is further enhanced to benzylic alcohols in DMF[25]. More recently, alcohol oxidation to aldehyde and ester through zinc (II) catalyst has also been reported (Scheme 1) where H_2O_2 is used as the terminal oxidant[26].

The zinc catalysis, in general, is not well explored compared to other transition metal catalysis[27]; however, a shift in the trend has been observed recently. Importance of zinc catalysis has been demonstrated in several recent reports, including oxidative

[a] *Department of Chemistry, COMSATS Institute for Information Technology, Campus Abbottabad, Abbottabad, Pakistan*

[b] *Leibniz-Institut für Katalyse e. V. an der Universität Rostock, Albert-Einstein-Str. 29a, 18059 Rostock, Germany*

[c] *Department of Physical Chemistry, University of Rostock, Dr.-Lorenz-Weg 1, 18059 Rostock, Germany*

[a] *Fax = +92-992-383441 khurshid@ciit.net.pk.*

† Footnotes relating to the title and/or authors should appear here.

Electronic Supplementary Information (ESI) available: Total electronic, zero-point and Gibbs free energies alongwith the cartesian coordinates of the optimized geometries are shown in the supplementary information. Supplementary data associated with this article can be found, in the online version,See DOI: 10.1039/x0xx00000x

transformations. The oxidation of alcohols to aldehydes and esters is achieved with zinc bromide and H_2O_2 as catalyst and oxidant, respectively [26] In a similar approach, aromatic aldehydes were previously converted to esters through zinc catalysis.[28] Zinc mediated oxidation of ether to aldehydes is also an interesting transformation [29]. Although experimental reports have started to emerge; however, the literature reveals only a handful number of theoretical mechanistic studies on zinc catalyzed reactions. More particularly, there appears no theoretical reports on the mechanism of any Zn(II) mediated oxidation reactions. A theoretical mechanistic study of the zinc(II) catalyzed oxidation of alcohols to aldehydes and esters under H_2O_2 and pyridinde-2-carboxlyic acid ligand is presented here. A main interest behind this study is to compare the mechanism of the zinc catalyzed reaction with other metals (ruthenium and other related metals).

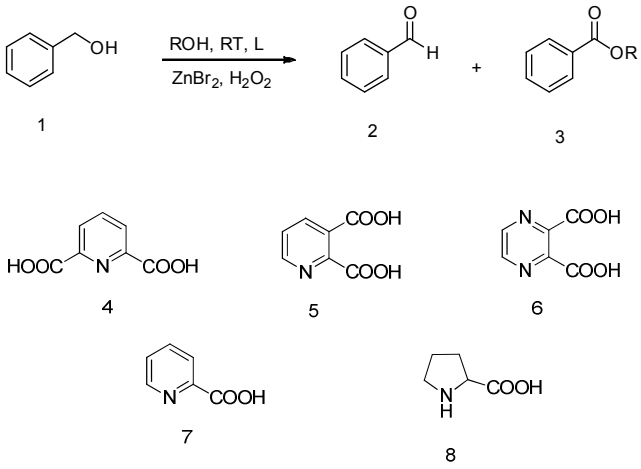

Scheme 1. Schematic presentation of zinc catalyzed oxidation of alcohols to esters

Computational methods

All calculations were performed with Gaussian 09.[30] Geometries of the structures were optimized without any symmetry constraints at hybrid B3PW91 using 6-311G(d,p)[31] basis set for C,H,N and oxygen, and SDDALL pseudopotential[32] for Zn, Br and I, unless otherwise noted. The B3PW91 method which consists of three parameter hybrid functional of Becke[33] in conjunction with the gradient corrected correlation functional of Perdew and Wang[34] was chosen since it has been shown to reliably model the similar oxidative reaction using Ru metal.[35] Each optimized structure was confirmed by frequency analysis at the same level to confirm the stationary point as a true minimum (no imaginary frequency) or a transition state (with one imaginary frequency). Intrinsic reaction coordinates (IRC) calculations were performed to confirm that the transition states connect to the right starting materials and products. IRC was performed until the stationary point was reached with RMS gradient less than 1 x 10^{-4} hartree/bohr. Stationary points located through IRC were then completely optimized at the above mentioned method. The solvent effect was studied through single point energy calculations in methanol solvent through polarization continuum model (PCM). The reported energies for all structures are Gibbs free energies (in kcal mol^{-1}).

Results and Discussion

To explore possible reaction mechanisms for the formation of **3** and **2** from **1**, we have performed DFT calculations at B3PW91 level of theory. Theoretical studies on oxidative esterification and amidation with other late transition metals (Ru, Pd, Au) reveal the occurrence of three possible mechanism; inner sphere, outer sphere and intermediate sphere mechanisms[36–46]. In inner sphere mechanism, a coordinated alcohol delivers a β hydride to metal (Figure 1). In the outer sphere mechanism,[47] the alcohol delivers a hydride to the metal, but without being coordinated to the metal. Both, inner sphere and outer sphere mechanisms involve the transfer of hydride to metal, however, in intermediate sphere mechanism; hydrogen is transferred to a hydrogen acceptor, instead of a metal.

Inner sphere mechanism involving liberation of hydrogen is proposed in the oxidative esterification by ruthenium pincer complex (Figure 1). An inner sphere mechanism is proposed for the palladium catalyzed esterification as well[48] However, a bifunctional double hydrogen transfer mechanism is shown to operate for ruthenium dehydrogenation catalyst[49] , originally discovered by Milstein[13]. Both, inner and outer sphere mechanism are shown to operate in the conversion of aliphatic amino alcohols to amino aldehydes.[50] Inner and outer sphere mechanisms involve a hydride abstraction by metal (vide supra). β-hydride elimination by metal requires a vacant coordination site and an electron in d orbital of metal. Considering these requirements, zinc species with more than three ligands is not anticipated as an active catalyst for β-hydride elimination. With these facts, it would be interesting to explore the operating mechanism in zinc catalysed oxidation reactions.

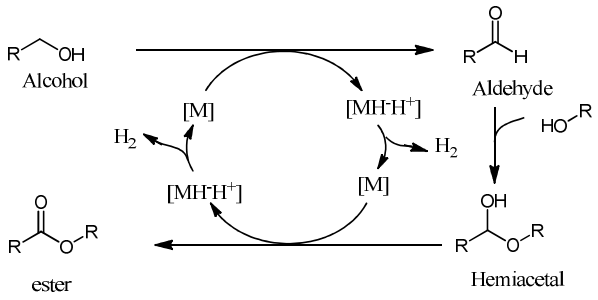

Figure 1. Catalytic cycle for metal [Ru] catalyzed dehydrogenative ester formation

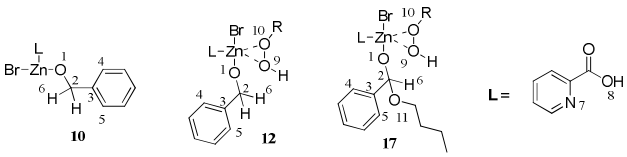

R=H for **12** and **17**

Figure 2. Numbering scheme for discussion of the computational results

Since the experimental reaction conditions show that the oxidative esterification reaction may be carried out in $ZnBr_2$ alone, without any added ligand, but the yields are low. Addition of ligands **4-8** significantly improves the conversion yields. Efficiencies of ligand **4** and **7** are much better than **5, 6** and **8**. Since the efficiencies of ligand **4** and **7** are comparable therefore, to reduce the computational cost, ligand **7** is used for this study. In the study by Wu, H_2O_2 is used as the oxidant. In a similar report, on oxidative amide formation from alcohol and amine, ZnI_2 and TBHP are used as the catalyst and oxidant, respectively. In this work, mechanistic details of $ZnBr_2$ catalyzed reaction in the presence of H_2O_2 oxidant are studied, and then, the effect of ligand, oxidant and catalyst are also explored.

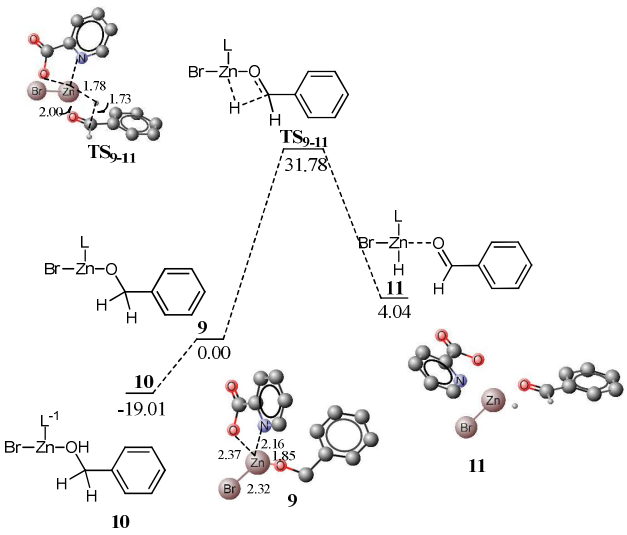

Figure 3. Energy profile for oxidation of alcohol to aldehyde through β hydride elimination (inner sphere mechanism) by zinc catalyst, calculated at B3PW91/6-311G(d,p) with SDDALL pseudo potential for Zn and Br. All energy values are relative to **9** at 0 kcal mol^{-1}. All bond lengths are in Angstroms. Unnecessary hydrogen atoms are removed for clarity

Initially, we studied inner sphere mechanism for zinc catalysed oxidation of alcohol to ester (Figure 3). The complex **9** is an eighteen electron complex, and has a distorted tetrahedral geometry around the zinc atom. . The complex **9** has another isomer **10** which is lower in energy than **9** by 19.01 kcal mol^{-1}. A proton from carboxylic oxygen (O8) in **9** is shifted to O1 in complex **10**. The complex **10** is occasionally obtained during the optimization of complex **9**.

A transition state $\mathbf{TS_{9\text{-}11}}$ for β hydride elimination by zinc is located at a barrier of 31.78 kcal mol^{-1} from **9**. This activation barrier is considerably higher than the one reported for the Ruthenium based catalyst (8.80 kcal mol^{-1})[49,50]. The high activation barrier is not unexpected because, the ability of transition metals to abstract a β-hydride decreases from left to right in the periodic table and it is expected to be small for zinc. There are certain marked differences in the transition states for Ru and zinc based species. The transition state for β hydride elimination to ruthenium catalyst is a very early transition state with geometry very similar to the starting material[50] whereas the zinc based transition state is almost middle. The geometry around zinc, in the transition state, is close to distorted square pyramid. The C2-H6 bond is considerably elongated to 1.73 Å in the transition state from 1.10 Å in **9**. Moreover, the Zn-H6 and O-Zn bond distances are 1.69 Å and 2.13 Å, respectively. A few important structural parameters are given in Table 1. The geometry around zinc in **11** is distorted tetrahedron. The aldehyde product is no longer in coordination with the metal centre. The aldehyde product shows hydrogen bonding interaction with the carboxylic acid moiety of the ligand. N7-Zn-H6, O1-Zn-O8 and N7-Zn-O8 bond angles are 116.24, 113.35 and 72.15 degrees, respectively. The hydride shift on zinc is also thermodynamically uphill by 4.04 kcal mol^{-1} from **9**. The kinetic barrier for the hydride elimination is much higher than the similar reaction with other late transition metals (vide supra) which may be attributed the electron rich nature of the zinc metal especially with four ligands coordinated. Since the reaction is carried out experimentally at room temperature, but the kinetic barrier for β hydride elimination

Table 1. Selected bond lengths of **9, 11** and $\mathbf{TS_{9\text{-}11}}$. All values are given in Angstroms

Bond	**9**	$\mathbf{TS_{9\text{-}11}}$	**11**
C-H	1.10	1.73	5.11
Zn-H	3.08	1.69	1.54
Zn-O	1.84	2.13	4.16
C-O	1.40	1.27	1.22

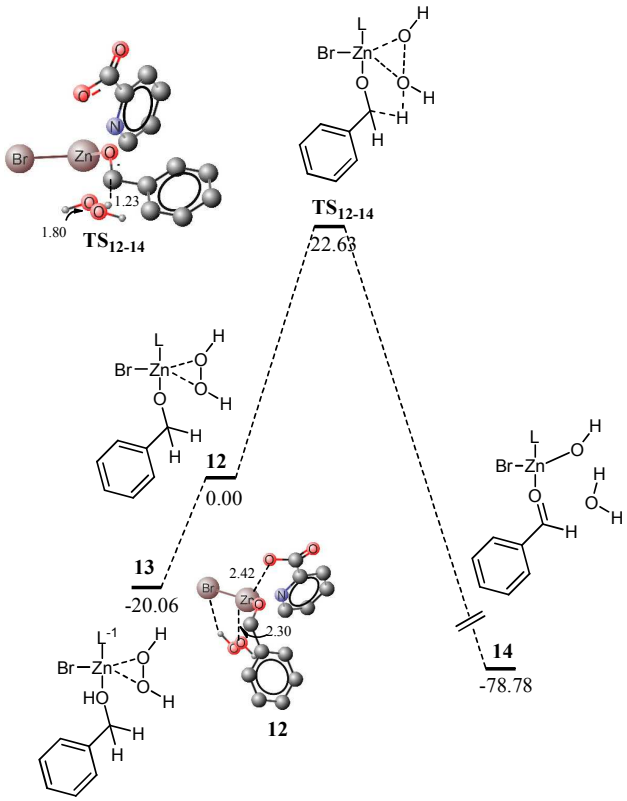

Figure 4. Energy profile for oxidation of alcohol to aldehyde through H_2O_2 coordinated to zinc catalyst, calculated at B3PW91/6-311G(d,p) with SDDALL pseudo potential for Zn and Br. All energy values are relative to **12** at 0 kcal mol^{-1}. All bond lengths are in Angstroms. Unnecessary hydrogen atoms are removed for clarity

is too high to be accessible under the reaction conditions. Therefore, β hydride elimination (inner sphere) is not believed as a plausible mechanism.

The inner sphere mechanism has too high kinetic barrier to be accessible under the experimental reaction conditions; therefore, intermediate sphere mechanism is envisaged. In the intermediate sphere mechanism, hydrogen acceptor (H_2O_2 in this case) also coordinates to the metal. The complex **12** is a 20 electron species with a distorted square pyramid type structure. The alkoxide oxygen (O1) is strongly coordinated to zinc at the distance of 1.87 Å. An oxygen atom of H_2O_2 (O9) is weakly coordinated to zinc (2.30 Å), but this interaction is strong compared to the coordination of carboxylic oxygen with zinc (2.42 Å). The other OH (O10) proton of H_2O_2 interacts with the bromide ligand. Quite similar to complex **9**, a proton shifted isomer of **12** is more stable than the complex 12. The complex **13** is structurally similar to **12** except that a proton from O8 is shifted to O1. The complex **13** is 20.06 kcal mol^{-1} more stable than **12**, and this energy difference is very similar to the difference in energies of **9** and **10** (19.01 kcal mol^{-1}).

A transition state for the hydrogen shift to hydrogen peroxide is located at a barrier of 22.63 kcal mol^{-1}. The kinetic barrier is remarkably lower, and easily accessible under the reaction conditions than the kinetic barrier for the inner sphere mechanism (31.78 kcal mol^{-1}). In the transition state, C2-H6 and O9-O10 bonds are elongated to 1.23 and 1.80 Å, respectively. Moreover, both oxygens of H_2O_2 are now coordinated to Zinc (2.28 and 2.66 Å). This additional interaction with zinc is probably responsible for the low activation barrier for the intermediate sphere mechanism. An *ortho* hydrogen of the pyridine moiety also shows interaction with O10 of H_2O_2 (2.06 Å). The reaction is thermodynamically favourable by 78.78 kcal mol^{-1} from **12**. The high energy of reactions may be due to several factors; the weak O9-O10 bond in the starting complex **13** is replaced by strong O-H bond, and OH moiety, generated during the reaction, is also coordinated to the metal.

The product of the reaction (**14**), is a penta coordinate complex. The water molecule produced (by the acceptance of hydrogen by H_2O_2) shows hydrogen bonding interactions with the OH ligand and the aldedhyde fragment. The water molecule acts as a hydrogen bond acceptor and donor for aldehyde (2.13 Å) and OH (1.71 Å) ligands, respectively. The OH group of the carboxylic acid has very weak interaction with the metal, and the bond is elongated to 2.42Å (see Figure 4 for details). The N7-Zn and O-Zn bond distances are 2.18 and 2.13 Å, respectively. The kinetic barrier predicted through this mechanism is in nice agreement with the experiment which suggests that intermediate sphere mechanism may be a plausible one. Another experimental aspect to support this mechanism is the acceleration of the reaction with higher concentration of H_2O_2, and it may be due to the direct involvement of H_2O_2 in the rate determining step (*vide supra*).

In similar reactions with other metals, an accepted notion is that the aldehyde generated reacts with alcohols to generate hemiacetals. The latter then enters into the catalytic cycle again and generates the ester product through another oxidation. Oxidation of aldehydes to esters is carried out with a variety of alcohols[26,28] for structural diversity in esters, however we have chosen butanol as an example. Formation of hemiacetal and its coordination to zinc by replacing water molecule is not analyzed in this study. In the intermediate sphere mechanism, the next step is the exchange of a proton with hydroxyl ligand to form alkoxy ligand. Although the proton exchange is not believed to a kinetically demanding step, but this reaction is modelled as well. The substrate may have many possible conformations and orientations of the aliphatic chain on oxygen with respect to the catalyst. A systematic search of all the possibilities in the intermediates and transition states is not carried out because they are not expected to significantly influence the energy profiles. The himiacetal bound complex **15** has a tetrahedral geometry around zinc. The hemiacetal oxygens are not coordinated with zinc in **15**, rather the hemiacetal is held there by hydrogen bonding interactions with other ligands (OH and L).The OH of hemiacetal has hydrogen bonding interaction with the hydroxyl ligand on Zn (O-H ---O bond distance is 1.56 Å). The O11 of the hemiacetal interacts with carboxylic oxygen (O10) at a distance of 1.61 Å. The Zn-Br distance in the complex is very similar to other

complexes (2.46 Å). Zn-O (OH), Zn-N7 and Zn-O8 bond distances are 1.93, 2.16 and 2.20 Å, respectively

All attempts to locate a transition state for proton shift in **15** met with failure. It may be argued that the proton shift may be a barrier less process, at least at this level of theory. Alternatively, it may be argued that the transition state for this reaction resides on a shallow potential energy surface and soon relaxes to either reactant or product for the reaction. The proton shift is a thermodynamically an uphill process by 5.35 kcal mol^{-1}. Surprisingly, a transition state for proton shift could be located at a barrier of 6.62 kcal mol^{-1} from **15** when lower level of theory was applied (B3PW91/6-31G(d) (for C, H, N and O) and LANL2DZ (Br and Zn). Most of the structural parameters remain constant on going from **15** to the transition state, $\mathbf{TS_{15\text{-}16}}$ except oxygen hydrogen bond distances at the active site.

Hemiacetal coordinated to zinc can be converted to an ester in a process very similar to the conversion of **12** to **14** (Figure 4). A transition state for intermediate sphere mechanism is modelled for this oxidation. Complex **17** is the active species for this reaction, generated by replacement of a water molecule in **16** with hydrogen peroxide. A transition state for the oxidation of hemiacetal to ester is located at a barrier of 21.99 kcal mol^{-1}. The structural features of the transition state are very similar to $\mathbf{TS_{12\text{-}14}}$. A few important structural features are given in Figure 5. The reaction is highly exothermic by 90.15 kcal mol^{-1}, and the exothermicity is even higher than that for **12** to **14**.

Kinetic barriers for the intermediate sphere mechanisms (Figure 4 and 5) are very consistent with the experimental reaction conditions which suggest that the intermediate sphere mechanism is a plausible mechanism for the conversion of alcohols into ester through zinc catalysis. Outer sphere mechanism is another possibility besides inner and intermediate sphere mechanism. However, the outer sphere mechanism is not investigated primarily because of two reasons: (a) the outer sphere mechanism also involves a hydride shift to zinc, which is believed to be kinetically highly unfavourable (very similar to inner sphere mechanism) because it involves a hydride shift to an electron rich zinc atom (b) the outer sphere mechanism also requires a proton acceptor at a suitable position, which is missing in this catalytic system.

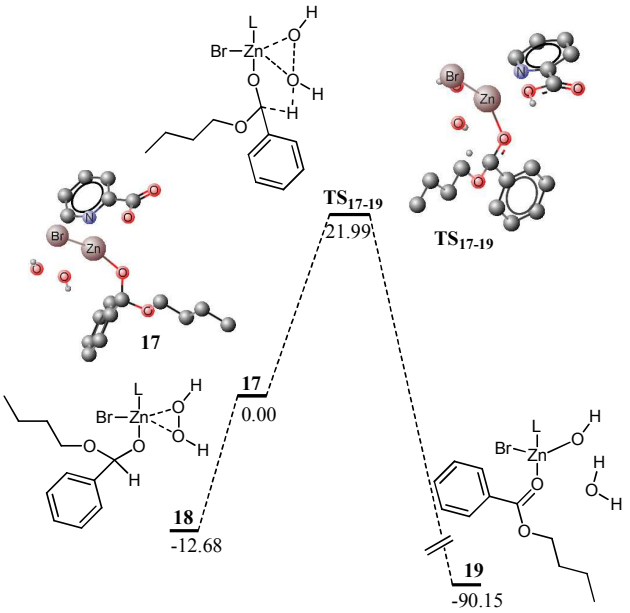

Figure 5. Energy profile for oxidation of hemiacetal to ester through H_2O_2 coordinated to zinc catalyst, calculated at B3PW91/6-311G(d,p) with SDDALL pseudo potential for Zn and Br. All energy values are relative to **17** at 0 kcal mol^{-1}. Unnecessary hydrogen atoms are removed for clarity

A number of zinc mediated oxidative transformation are recently reported in the literature where variation in zinc halides (ZnI_2, $ZnBr_2$, $ZnCl_2$), oxidant (TBHP, H_2O_2) and ligands have been studied. Some of these reactions involve significant changes in the catalytic system. For example, ZnI_2 and TBHP are used as the catalyst and oxidant, respectively in the oxidative transformation of alcohol and amines to amides without any added ligand. Therefore, in this study, effect of oxidant and zinc catalyst is studied and finally the kinetics and thermodynamics of ligand less reaction are also investigated. In the first approach, effect of oxidant is investigated where H_2O_2 is replaced with TBHP, and the potential energy diagram for intermediate sphere mechanism is explored. The potential energy for inner sphere mechanism is not affected with changes in the oxidant because oxidant is not involved in the β hydride elimination. The potential energy diagram for the oxidation of alcohol to ester with TBHP (through intermediate sphere mechanism) is very similar to H_2O_2 mediated reaction. Replacement of a hydrogen atom with a *tert*-butyl group does not cause significant changes in the geometry of complex **20**. The interaction of the hydroxyl proton O10 (of H_2O_2) with the bromide ligand causes some deformation of geometry of the complex **12** (Figure 6)**.** The geometries and related structural parameters are shown in Figure 6.

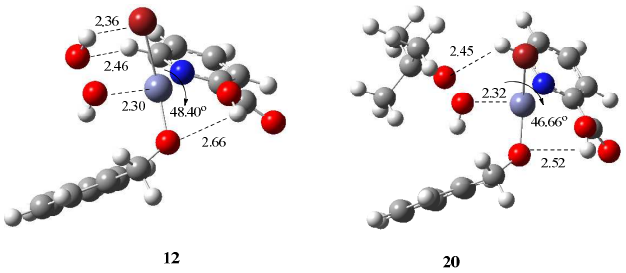

Figure 6. Optimized geometries and related structural parameters for **12** and **20**

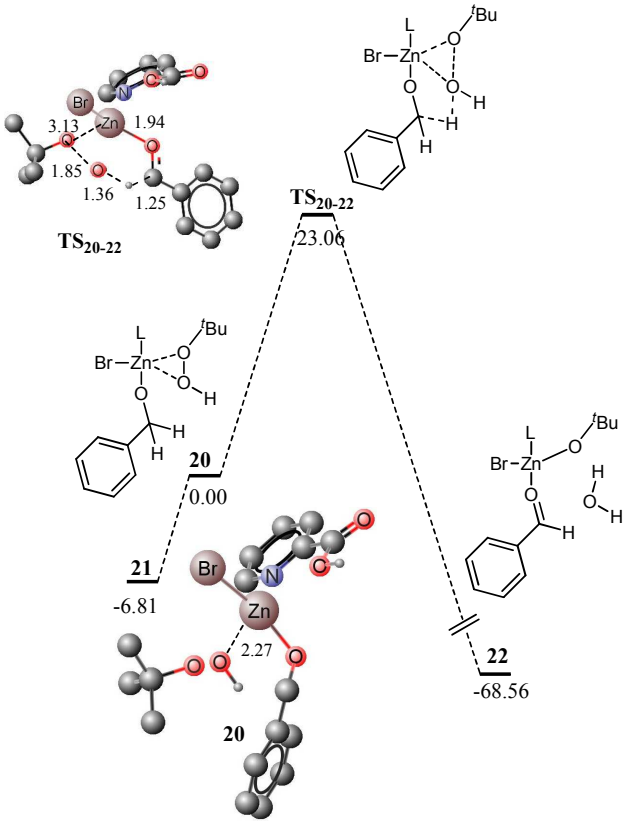

Figure 7. Energy profile for oxidation of alcohol to aldehyde through TBHP coordinated to zinc catalyst, calculated at B3PW91/6-311G(d,p) with SDDALL pseudo potential for Zn and Br. All energy values are relative to **20** at 0 kcal mol^{-1}. All bond lengths are in Angstroms. Unnecessary hydrogen atoms are removed for clarity

Structure **21** is an isomer of compound **20** which lies about 6.81 kcal mol^{-1} lower in energy than **20** (Figure 7). In **21**, the benzyloxy moiety does not show hydrogen bonding interaction with the carboxylic acid part of the ligand, rather it shows non-bonding interactions with the OH of TBHP. Activation barrier for the oxidation to aldehyde through TBHP oxidant was calculated at 23.06 kcal mol^{-1}. The activation barrier with TBHP is slightly higher than the corresponding reaction with H_2O_2 (22.63 kcal mol^{-1}). Changing the oxidant from H_2O_2 to TBHP affects the interactions in the transition states, as well. With H_2O_2, the hydroxyl (O10) proton shows non-bonding interactions with the bromide ligand whereas with TBHP, a proton form the tertiary butyl group shows non-bonding interaction with bromide. Most of the other structural features are very similar for both transition states except C2-H6 and Zn-OBu/OH bond distances. These distances are small with H_2O_2. These small distances probably make the **TS_{12-14}** more stable than **TS_{20-22}**. The reaction is highly exothermic, quite similar to the reaction with H_2O_2. Energy profile for proton shift in **23** to deliver **24** is very similar to what is observed for the transformation of **15** to **16**. The transition state could not be located at higher level of theory; however, it could be located at a lower level (Figure S1 and S2).

Hydrogen transfer from hemiacetal to TBHP in **25** (to deliver the ester complex **26)** (Figure S3) has a kinetic barrier of 18.75 kcal mol^{-1}, which is lower than the oxidation of benzylic alcohol to benzladehyde under TBHP conditions (**TS_{20-22}**). This trend is consistent with what is observed with H_2O_2, i.e., activation barriers for oxidation of hemiacetal to esters are lower than the oxidation of benzylic alcohols to aldehydes; however, the activation barrier is much lower with TBHP. The kinetic barrier for the oxidation to esters with TBHP is about 3.24 kcal mol^{-1} lower than with H_2O_2. A comparison of the energy profiles for reactions under TBHP and H_2O_2 conditions illustrate that H_2O_2 is a better oxidant in intermediate sphere mechanism for the oxidation to aldehydes whereas TBHP is superior for oxidation to esters. These theoretical findings are consistent with the experimental observation[33].

To explore the effect of halide ligands on zinc, TBHP coordinated complexes are analysed. Hydrogen transfer from the zinc iodide coordinated benzylic alcohol **27** to generate benzaldehdye **28** (Figure S4) is kinetically less demanding by 4.70 kcal mol^{-1} than the similar reaction in **20**. However, an increase in activation barrier for the ester formation step is observed (21.53 kcal mol^{-1}). The transition state from **29** lies at a barrier of 21.53 kcal mol^{-1} compared to 18.75 kcal mol^{-1} from **25**. These theoretical calculations are in accordance with the practical observations. Under similar conditions, 61% conversion has been observed experimentally with $ZnBr_2$ whereas only 50% conversion is reached with ZnI_2. Moreover, for ZnBr2, ester is the dominant product whereas ZnI2 delivers only aldehyde product. The oxidation of aldehyde to ester using ZnI2 is hindered by the higher activation barrier for the second oxidations step (See Figure S5).

Finally, the effect of the ligand (pyridine-2-carboxylic acid) on the oxidative esterification is explored. Since the zinc complex without the pyridine-2-carboxylic acid ligand is less than 18 electron species therefore it is interesting to investigate whether β hydride elimination is a favourable process in these complexes or not. Activation barrier for the hydride shift is about 30.94 kcal mol^{-1} with respect to **30a**. The activation barrier for the hydride shift is

relatively decreased in the absence of the ligand (30.94 vs. 31.78 kcal mol^{-1}) (See Figure S6) In the transition state (TS_{30a-31}), C2-H and Zn-H bond lengths are 1.62 and 1.68 Å respectively. Moreover, the reaction is thermodynamically uphill. The product of this step **31** lies 6.23 kcal mol^{-1} higher in energy than **30a**.

Since the activation barriers associated with the inner sphere mechanism (shown in Figure S6) are slightly decreased in the absence of ligand (although highly inaccessible at room temperature), it was of great interest to investigate the energetics of ligand less intermediate sphere mechanism. A transition state was located for a hydrogen shift to TBHP with concomitant breakage of O-O bond at barrier of 29.37 kcal mol^{-1} from **32a**. In the transition state, C1-H8 and H8-O6 bond lengths are 1.21 and 1.52Å, respectively. The O6-O7 bond of TBHP is considerably elongated (1.81Å compared to 1.44Å. in **32a**). The transition state is of relatively lower energy compared to the one for hydride shift to zinc, and the overall reaction is highly exothermic. The activation barrier for hydrogen shift to TBHP in the absence of ligand is about 7 kcal mol^{-1} higher than with the ligand. This is again consistent with the experimental observation where 100% conversions were achieved in the presence of ligand compared to 50-60% conversion in the absence of ligand. Although the activation barrier for intermediate sphere mechanism is increased in the absence of ligand, but the activation barrier is yet lower than for the inner sphere mechanism (β hydride elimination). These calculations reveal that, intermediate sphere mechanism is the plausible mechanism, in the presence and absence of ligands. The water molecule generated as a result of hydrogen shift also coordinates with the zinc atom although this oxygen atom is quite away from zinc in the starting material **32a** (compare 2.30Å in TS_{32a-33} with 2.91 Å in **32a**). The low activation barrier may be attributed (Figure S7) to the formation of metal oxygen bond in the transition state compared to relatively unstable M-H bond in the TS_{30a-31}.

Conclusions

In summary, mechanism of the zinc (II) catalyzed oxidative transformation of alcohols to ester through H_2O_2 oxidant is investigated by density functional theory methods, and the mechanistic outcomes are compared with those of other late transition metals. Both, inner sphere and intermediate sphere mechanisms have been analyzed in the presence and absence of pyridine-2- carboxylic acid (ligand). The inner sphere mechanism which involves a hydride transfer to the transition metal is found kinetically more demanding than the competitive intermediate sphere mechanism. In the presence of the ligand, the calculated activation barrier for β hydride elimination (inner sphere) is 31.78 kcal mol^{-1}. The calculated activation barriers for hydrogen shift from the alkoxy ligand (intermediate sphere mechanism) to oxidant (H_2O_2) are 22.63 and 21.99 kcal mol^{-1} for aldehyde and ester formation steps, respectively. Ligands significantly affect the inner and intermediate sphere mechanisms. In the absence of ligand (pyridine-2-carboxylic acid), the activation barrier for β hydride elimination increases slightly. However, the effect is more pronounced for intermediate sphere mechanism where activation barrier for the rate determining step decreases by more than 7 kcal mol^{-1}. The effect of halide (on zinc) is relatively small. Presence of an iodide on zinc instead of a bromide provides an easy access to aldehydes because of lower activation barrier for the first step whereas the activation energy for the second step is significantly increased. Moreover, steric bulk in the oxidant such as TBHP increases the activation barrier for the oxidation of alcohols to esters by 0.43 kcal mol^{-1}; however, the activation barrier for oxidation of hemiacetals to esters is reduced by 3.24 kcal mol^{-1}. The mechanism of zinc catalyzed oxidative esterification is different from the mechanism of the same reaction with other late transition metals. In Ru, Pd and Ir where inner or outer sphere mechansims operate, the intermediate sphere mechanism for zinc is an interesting aspect for further exploration in the area

Acknowledgements

The authors acknowledge the financial support from Higher Education Commission of Pakistan (Grant No. 1899), COMSATS Institute of Information Technology, and University of Rostock. This work has been partly supported by the BMBF within the project "Light2Hydrogen" (Spitzenforschung und Innovation in den Neuen Landern), by the European Union (European Social Funds, ESF) within the project "PS4H" and by the Ministry for Education, Science and Culture of Mecklenburg-Vorpommern.

Notes and references

(1) Otera, J. *Esterification: Methods, Reactions, and Applications*; WileyVCH: Weinheim, 2003.

(2) *Modern Polyester: Chemistry and Technology of Polyester and Copolyesters*; Scheirs, J., Long, T. E., Eds.; WileyVCH, 2003.

(3) Larock, R. C. *Comprehensive Organic Transformations: A Guide to Functional Group Preparations, 2nd ed.*; Wiley-VCH: New York, USA, 1999.

(4) Finkelstein, H. *Berichte der Dtsch. Chem. Gesellschaft* **1910**, *43*, 1528–1532.

(5) Perkowski, A. J.; Nicewicz, D. A. *J. Am. Chem. Soc.* **2013**, *135*, 10334–10337.

(6) *Compendium of Organic Synthetic Methods*; Harrison, I. T., Harrison, S., Eds.; Compendium of Organic Synthetic Methods; John Wiley & Sons, Inc.: Hoboken, NJ, USA, 1971; Vol. 1.

(7) Brennführer, A.; Neumann, H.; Beller, M. *Angew. Chem. Int. Ed. Engl.* **2009**, *48*, 4114–4133.

(8) Rout, S. K.; Guin, S.; Ghara, K. K.; Banerjee, A.; Patel, B. K. *Org. Lett.* **2012**, *14*, 3982–3985.

(9) Wu, X.-F.; Darcel, C. *European J. Org. Chem.* **2009**, *2009*, 1144–1147.

(10) Gowrisankar, S.; Neumann, H.; Beller, M. *Angew. Chem. Int. Ed. Engl.* **2011**, *50*, 5139–5143.

(11) Liu, C.; Wang, J.; Meng, L.; Deng, Y.; Li, Y.; Lei, A. *Angew. Chem. Int. Ed. Engl.* **2011**, *50*, 5144–5148.

(12) Guerbet, M. C. R. *Acad. Sci. Paris* **1899**, *128*, 1002.

(13) Zhang, J.; Leitus, G.; Ben-David, Y.; Milstein, D. *J. Am. Chem. Soc.* **2005**, *127*, 10840–10841.

(14) Dobereiner, G. E.; Crabtree, R. H. *Chem. Rev.* **2010**, *110*, 681–703.

(15) Bai, X.-F.; Ye, F.; Zheng, L.-S.; Lai, G.-Q.; Xia, C.-G.; Xu, L.-W. *Chem. Commun. (Camb).* **2012**, *48*, 8592–8594.

(16) Liu, C.; Tang, S.; Lei, A. *Chem. Commun. (Camb).* **2013**, *49*, 1324–1326.

(17) Oliveira, R. L.; Kiyohara, P. K.; Rossi, L. M. *Green Chem.* **2009**, *11*, 1366.

(18) Miyamura, H.; Yasukawa, T.; Kobayashi, S. *Green Chem.* **2010**, *12*, 776.

(19) Gunanathan, C.; Shimon, L. J. W.; Milstein, D. *J. Am. Chem. Soc.* **2009**, *131*, 3146–3147.

(20) Yamamoto, N.; Obora, Y.; Ishii, Y. *J. Org. Chem.* **2011**, *76*, 2937–2941.

(21) Su, F.-Z.; Ni, J.; Sun, H.; Cao, Y.; He, H.-Y.; Fan, K.-N. *Chemistry* **2008**, *14*, 7131–7135.

(22) Nielsen, M.; Junge, H.; Kammer, A.; Beller, M. *Angew. Chem. Int. Ed. Engl.* **2012**, *51*, 5711–5713.

(23) Zhao, J.; Mück-Lichtenfeld, C.; Studer, A. *Adv. Synth. Catal.* **2013**, *355*, 1098–1106.

(24) Wang, L.; Li, J.; Dai, W.; Lv, Y.; Zhang, Y.; Gao, S. *Green Chem.* **2014**.

(25) Zhu, Y.; Wei, Y. *European J. Org. Chem.* **2013**, *2013*, 4503–4508.

(26) Wu, X.-F. *Chemistry* **2012**, *18*, 8912–8915.

(27) Enthaler, S. *ACS Catal.* **2013**, *3*, 150–158.

(28) Wu, X.-F. *Tetrahedron Lett.* **2012**, *53*, 3397–3399.

(29) Song, Z.-Z.; Gong, J.-L.; Zhang, M.; Wu, X.-F. *Asian J. Org. Chem.* **2012**, *1*, 214–217.

(30) Frisch, M. J.; Trucks, G. W.; Schlegel, H. B.; Scuseria, G. E.; Robb, M. A.; Cheeseman, J. R.; Scalmani, G.; Barone, V.; Mennucci, B.; Petersson, G. A. *Wallingford CT* **2009**.

(31) Hariharan, P. C.; Pople, J. A. *Theor. Chim. Acta* **1973**, *28*, 213–222.

(32) Dunning, T. H.; Hay, P. H. *Modern Theoretical Chemistry*; Schaefer, H. F., Ed.; New York, USA, 1976.

(33) Becke, A. D. *J. Chem. Phys.* **1993**, *98*, 5648.

(34) Perdew, J. P. *Electronic structure of Solids*; Ziesche, P., Eschrig, H., Eds.; Akademic Verlag: Berlin, 1991.

(35) Nova, A.; Balcells, D.; Schley, N. D.; Dobereiner, G. E.; Crabtree, R. H.; Eisenstein, O. *Organometallics* **2010**, *29*, 6548–6558.

(36) Zassinovich, G.; Mestroni, G.; Gladiali, S. *Chem. Rev.* **1992**, *92*, 1051–1069.

(37) Samec, J. S. M.; Bäckvall, J.-E.; Andersson, P. G.; Brandt, P. *Chem. Soc. Rev.* **2006**, *35*, 237–248.

(38) Noyori, R. Asymmetric catalysis: Science and opportunities (nobel lecture). *Angewandte Chemie - International Edition*, 2002, *41*, 2008–2022.

(39) Bullock, R. M. *Chemistry - A European Journal*, 2004, *10*, 2366–2374.

(40) Clapham, S. E.; Hadzovic, A.; Morris, R. H. *Coordination Chemistry Reviews*, 2004, *248*, 2201–2237.

(41) Ikariya, T.; Blacker, A. J. *Accounts of Chemical Research*, 2007, *40*, 1300–1308.

(42) Ikariya, T. *Top. Organomet. Chem.* **2011**, *37*, 31–53.

(43) Nixon, T. D.; Whittlesey, M. K.; Williams, J. M. J. *Dalton Trans.* **2009**, 753–762.

(44) Eisenstein, O.; Crabtree, R. H. *New Journal of Chemistry*, 2013.

(45) Conley, B. L.; Pennington-Boggio, M. K.; Boz, E.; Williams, T. J. *Chem. Rev.* **2010**, *110*, 2294–2312.

(46) Comas-Vives, A.; Ujaque, G.; Lledós, A. *Inner- and Outer-Sphere Hydrogenation Mechanisms: A Computational Perspective*; 2010; Vol. 62.

(47) Noyori, R.; Ohkuma, T. *Angew. Chem. Int. Ed.* **2001**, *40*, 40.

(48) Hu, W.; Li, J.; Deng, S.; Huang, J.; Le, X.; Zheng, W. *J. Organomet. Chem.* **2013**, *740*, 10–16.

(49) Cho, D.; Ko, K. C.; Lee, J. Y. *Organometallics* **2013**, *32*, 4571–4576.

(50) Nova, A.; Balcells, D.; Schley, N. D.; Dobereiner, G. E.; Crabtree, R. H.; Eisenstein, O. *Organometallics* **2010**, *29*, 6548–6558.

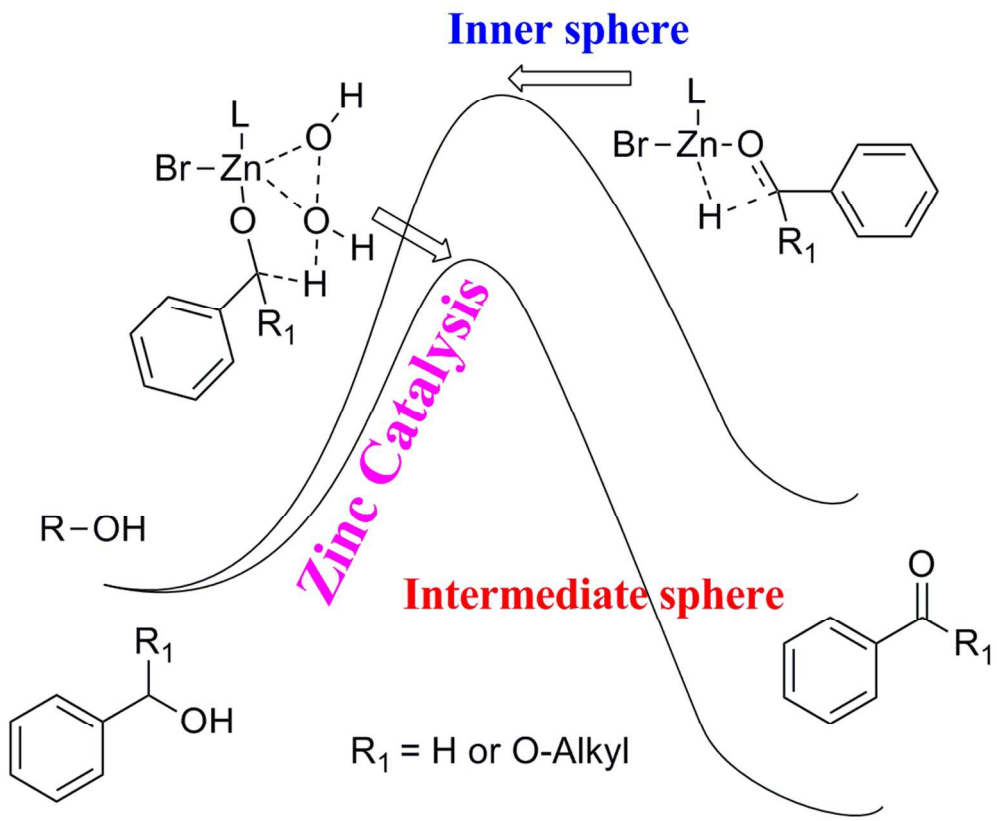

95x79mm (300 x 300 DPI)